

Magnetic and Crystal Structure of Titanium Sesquioxide

S. C. ABRAHAMS*

Bell Telephone Laboratories, Murray Hill, New Jersey

(Received 4 February 1963)

A single-crystal neutron diffraction study has been made of titanium sesquioxide in the temperature range 1.4 to 711°K. The crystal undergoes a transition at a temperature variously reported as about 450 to 600°K, below which the structure becomes antiferromagnetic. In the crystal studied, $T_N \approx 660^\circ\text{K}$. The magnetic moments in this corundum-type structure have an arrangement similar to that in α hematite between 253 and 948°K. Puckered sheets of Ti^{3+} , parallel to (111), are ferromagnetic with moments lying in the plane normal to the trigonal axis. Adjacent cation sheets, separated by a layer of oxygen, have antiparallel moments. The magnitude of the moment is about $0.2 \mu_B$ per Ti^{3+} . There is no evidence for a moment parallel to the trigonal axis. The magnetic form factor *increases* with scattering angle, due to some unquenched orbital momentum. An explanation for the observed form factor and for the moment perpendicular to [111] has been given by Blume. The density maxima of antiparallel pairs of moments are displaced toward each other along the trigonal axis.

INTRODUCTION

TITANIUM sesquioxide was first reported by Naylor¹ to undergo a transition. He observed a change in specific heat of about 215 cal mole⁻¹ at about 473°K.² Many other studies have since confirmed the existence of this transition. The magnetic susceptibility changes^{3,4} by about a factor of 2 in the temperature range 400 to 500°K, and the resistivity by as much as two orders of magnitude^{5,6}: In the latter case, the temperature range reported was about 350 to 700°K. The thermoelectric power⁶ also shows a clear break in the temperature range 450 to 600°K. Pearson⁴ has found no change in the Ti_2O_3 corundum-type structure in the temperature range 298 to 623°K, although the lattice parameters vary rapidly between 430 and 473°K.

Pearson⁴ and Morin^{5,7} have proposed that this transition is associated with a change from a paramagnetic to an antiferromagnetic state. This could account^{5,7} for the transition from metal to semiconductor at the Néel point as the $3d$ electrons in a narrow conduction band above T_N become localized in an antiferromagnetic array below T_N . Goodenough⁸ has suggested that below the transition temperature, a strong $\text{Ti}^{3+}-\text{Ti}^{3+}$ interaction will lead to direct bond formation between the cations along the trigonal axis. An attempt to observe the predicted antiferromagnetic ordering directly by neutron diffraction using a powder sample at 4.2°K and at 295°K was unsuccessful⁹: An upper limit of $0.5 \mu_B$ per Ti^{3+} was placed on the cation

moment. Some preliminary single-crystal work in the same report indicated the maximum but unobserved moment could be no more than $0.3 \mu_B$ per Ti^{3+} . This paper presents evidence for an antiferromagnetic ordering of small magnitude moment associated with the Ti^{3+} cations below a Néel temperature of about 660°K.

CRYSTAL DATA

Titanium sesquioxide, Ti_2O_3 ; formula weight = 143.80; $D_x = 4.57 \text{ g cm}^{-3}$; $D_m = 4.61 \text{ g cm}^{-3}$. Rhombohedral with $a = 5.433 \pm 0.001 \text{ \AA}$, $\alpha = 56^\circ 34' \pm 1'$ at 198°K.¹⁰ At 1.43°K, the lattice constants do not differ from those at 298°K by more than 0.5%. The variation in lattice constants between 298 and 623°K has already been reported.⁴ There are two formula weights per rhombohedral unit cell. Nuclear scattering indicated that (hll) is present only for $h=2n$, as found by x rays¹¹: (hkl) has no conditions. The nuclear space group is hence $D_{3d}^6 - R\bar{3}c$. Magnetic scattering indicates no change in unit cell dimensions but (hll) is observed present for $h=2n+1$. The most likely magnetic space groups are $C2/c$ or $C2'/c'$, in which the rhombohedral [111] (i.e., the hexagonal c axis) becomes the monoclinic c axis, the hexagonal a axis becomes the monoclinic b axis and the monoclinic a axis is given by the vector from the inversion center at the origin and terminating on the hexagonal lattice point with coordinates $\frac{2}{3}, \frac{1}{3}, \frac{1}{3}$. The corresponding monoclinic lattice constants are $a = 9.569$, $b = 5.149$, $c = 13.642 \text{ \AA}$, and $\alpha = 161^\circ 54'$. Absorption coefficient for neutrons with $\lambda = 1.032 \text{ \AA}$ is 0.135 cm^{-1} . Volume of the rhombohedral unit cell is 104.38 \AA^3 . Nuclear scattering lengths are $b_{\text{Ti}} = -0.38$, $b_{\text{O}} = 0.58 \times (10^{-12} \text{ cm})$.

EXPERIMENTAL

A cylindrical crystal with dimensions 2.69 mm in diameter and 4.78 mm in length was machined from a

¹⁰ R. E. Newnham, MIT Laboratory for Insulation Research Report No. 25, 1959, p. 39 (unpublished).

¹¹ This is equivalent to the condition that (hll) is present only for $l=2n$.

* Guest Scientist at Brookhaven National Laboratory, Upton, New York.

¹ B. F. Naylor, J. Am. Chem. Soc. **68**, 1077 (1946).

² This has recently been revised to 36 cal mole⁻¹ at 453°K by S. Nomura, T. Kawakubo, and T. Yanagi, J. Phys. Soc. Japan **16**, 706 (1961).

³ M. Foëx and J. Wucher, Compt. Rend. **241**, 184 (1955).

⁴ A. D. Pearson, J. Phys. Chem. Solids **5**, 316 (1958).

⁵ F. J. Morin, Phys. Rev. Letters **3**, 34 (1959).

⁶ J. Yahia and H. P. R. Frederikse, Phys. Rev. **123**, 1257 (1961).

⁷ F. J. Morin, Bell System Tech. J. **37**, 1047 (1958).

⁸ J. B. Goodenough, Phys. Rev. **117**, 1442 (1960).

⁹ G. Shirane, S. J. Pickart, and R. Newnham, J. Phys. Chem. Solids **13**, 167 (1960).

single-crystal boule of Ti_2O_3 purchased from the Linde Air Products Company, with the cylinder axis aligned within 1 deg of the rhombohedral $[\bar{1}10]$. After the final grinding, the cylinder was lightly etched to remove surface damage that had been observed by use of Laue x-ray photography. The integrated intensities of the diffracted neutron beams in the (hll) zone were measured using SCAND,¹² the single-crystal automatic neutron diffractometer at Brookhaven. Every reflection in this reciprocal lattice layer was measured at 4.2°K, within the limit of $\sin\theta/\lambda \leq 0.84 \text{ \AA}^{-1}$, including all equivalent reflections. Many individual intensities at this temperature were measured several times. The crystal was cooled and maintained at 4.2°K in the cryostat previously described.¹³ Some magnetic intensities were also measured with the crystal at 1.43°K by pumping on the liquid-helium reservoir in the cryostat to a pressure of 2.5 mm of mercury. Intensity measurements were made on the crystal at room temperature both with the cryostat-mounted crystal and also with the crystal mounted within an evacuated furnace.¹⁴ This furnace was used to raise the crystal temperature to 323, 373, 441, 477, 577, 631, 689, and 711°K. After each change in temperature, the crystal was required to be slightly reoriented: This was possible since the furnace was mounted on a large goniometer head.¹⁴ Selected reflections were measured at each of these temperatures. The ratio of the largest to the smallest integrated intensity, measured at 4.2°K, was 827:1.

The observation of (hll) reflections with $h=2n+1$ is not, without additional proof, unambiguous evidence of a magnetic interaction with the spin of the pile neutrons. There are three other possible sources for these nuclear space group forbidden reflections. One is the "simultaneous" or "unweganregung" reflection mechanism, often observed in neutron single-crystal diffractometry. The second is some "mistake" in the structure due, for example, to nonstoichiometry, resulting in a real departure from the normal corundum-type structure. The third is $\lambda/2$ reflection from the allowed nuclear reciprocal lattice points, which would occur as subharmonic reflections. Several of these "forbidden" reflections were hence measured as a function of rotation about their scattering vectors. The complete cryostat assembly was, thus, rotated through about 20° for (111), (100), and $(\bar{1}11)$, maintaining each reflecting plane normal to this rotation axis. The intensities of these reflections remained constant throughout the rotations, eliminating the "unweganregung" source. The possibility that this class of reflection is nuclear in origin was readily checked. A small fragment from the original boule was ground into a sphere of radius 0.2 mm. The (hll) reciprocal layer was photographed with MoK_α x rays, excited at a voltage too low to give a half-

TABLE I. Measured and calculated values of the titanium sesquioxide nuclear structure factors at 4.2°K.

hkl	F_{meas}	F_{calc}	hkl	F_{meas}	F_{calc}
011	0.32	0.28	611	0.93	-0.94
022	0.59	0.59	622	0.24	0.20
033	2.78	-4.24	633	1.92	1.93
044	0.97	0.93	644	0.27	-0.20
055	1.83	1.75	655	1.50	1.49
066	1.52	1.42	666	2.75	-2.86
200	0.95	1.00	677	0.69	-0.76
211	1.23	1.34	688	1.33	1.19
222	2.94	-4.71	822	1.49	1.39
233	0.23	0.17	833	0.28	0.31
244	1.62	1.70	844	1.97	1.86
255	1.97	1.93	855	2.50	-2.57
266	1.45	-1.44	866	1.27	-1.28
277	0.37	0.35	877	0.85	0.81
400	1.86	1.93	$\bar{2}11$	1.70	1.78
411	2.77	-4.24	222	0.64	-0.59
422	0.55	-0.55	$\bar{2}33$	<0.21	-0.03
433	1.06	1.11	$\bar{2}44$	2.76	-3.09
444	2.15	2.13	$\bar{2}55$	1.37	1.41
455	0.87	-0.88	$\bar{4}11$	1.35	1.30
466	0.88	0.90	$\bar{4}22$	1.31	1.30
477	2.39	-2.58	$\bar{4}33$	1.14	-1.23
600	2.81	-3.07	$\bar{6}11$	2.10	2.12

wavelength component, on a precession camera. Heavily exposed photographs showed no signs of reflections with $h=2n+1$, thus removing this as the source. The final possibility was effectively eliminated by use of a plutonium-foil filter. The ratio of a typical magnetic reflection to its second-order nuclear reflection such as $I(100):I(200)=1:52$ may be compared with that of a completely forbidden reflection to its second order, for example, $I(0,1\frac{1}{2},1\frac{1}{2}):I(033) < 1:567$. This demonstrates the effective absence of $\lambda/2$. The $h=2n+1$ reflections in (hll) , hence, may be regarded as magnetic in origin.

The resulting structure factors in (hll) for $h=2n$ are given in Table I under F_{meas} ; for $h=2n+1$ they are listed in Table II under F_{meas} . Both sets are on the same scale.

REFINEMENT OF THE CRYSTAL STRUCTURE AT 4.2°K

It was necessary to analyze the nuclear structure factors at 4.2°K and, hence, establish the absolute scale, before the magnetic structure factors could be considered on an absolute basis. Atomic coordinates at 298°K already determined by Newnham,^{10,15} using x-ray photography, as $u_{Ti} = 0.345 \pm 0.001$ and $v_0 = 0.567 \pm 0.005$, were used as starting values. In the rhombohedral space group $R\bar{3}c$, the Ti^{3+} is in the position $(4c)$ at uuu and the O^{2-} is in $(6e)$ at $v, \frac{1}{2}-v, \frac{1}{4}$, the origin being taken at the inversion center with point symmetry

¹² E. Prince and S. C. Abrahams, Rev. Sci. Instr. **30**, 581 (1959).

¹³ S. C. Abrahams, Rev. Sci. Instr. **31**, 174 (1960).

¹⁴ S. C. Abrahams, Rev. Sci. Instr. **34**, 113 (1963).

¹⁵ R. E. Newnham, MIT Laboratory for Insulation Research Report No. 26, 1960, p. 10 (unpublished).

TABLE II. Measured and calculated values of the titanium sesquioxide magnetic structure factors at 4.2°K.

<i>hkl</i>	F_{meas}	$F_{\text{calc}}(\text{a})$	$F_{\text{calc}}(\text{b})$	$F_{\text{calc}}(\text{a}-1)$
100	0.09	-0.10	0.14	-0.09
111	0.19	0.22	0.05	0.22
122	0.10	-0.04	-0.23	-0.10
133	0.17	-0.21	0.12	-0.14
144	0.19	0.23	0.18	0.28
155	<0.23	0.08	-0.28	-0.11
166	<0.23	-0.31	0.03	-0.19
300	0.14	0.20	0.04	0.20
311	0.13	-0.03	-0.22	-0.10
322	0.16	-0.21	0.13	-0.14
333	0.20	0.20	0.15	0.25
344	0.17	0.08	-0.27	-0.11
355	<0.16	-0.30	0.03	-0.18
500	<0.13	-0.04	-0.24	-0.11
511	0.20	-0.21	0.13	-0.14
522	0.14	0.21	0.16	0.26
533	0.19	0.08	-0.27	-0.11
544	0.21	-0.30	0.03	-0.18
555	0.26	0.14	0.28	0.31
566	<0.19	0.22	-0.25	-0.13
577	<0.20	-0.27	-0.10	-0.19
$\bar{1}11$	0.11	-0.10	0.15	-0.09
$\bar{1}22$	0.19	0.20	0.04	0.20
$\bar{1}33$	<0.14	-0.04	-0.23	-0.10
$\bar{1}44$	<0.15	-0.22	0.13	-0.15
$\bar{3}11$	0.15	-0.12	0.17	-0.11
$\bar{3}22$	<0.14	-0.13	0.19	-0.11
$\bar{3}33$	0.25	0.24	0.05	0.25
$\bar{3}44$	<0.19	-0.04	-0.28	-0.13
$\bar{5}11$	0.25	0.24	0.05	0.25
$\bar{5}22$	<0.21	0.15	0.21	-0.12

3. Initial refinement was by the method of least squares assuming isotropic temperature factors, using the ORXLS program¹⁶ and resulted in the values of Table III.

Additional cycles of least-squares refinement were then computed, with anisotropic temperature factors. The positional coordinates did not change significantly, but the ratio $\beta_{11}:\beta_{33}$ for Ti changed from 7.8:1 to 20.0:1 and for O from 6.5:1 to 5.4:1. The final coordinates are given in Table IV.

The course of the refinement may be followed by the value of R (defined as $\sum(|F_{\text{meas}}| - |F_{\text{calc}}|) / \sum(|F_{\text{meas}}|)$) at the various stages. Initially $R=0.312$, the coordinates in Table III correspond to $R=0.147$ and in Table IV to $R=0.117$. The latter value is reduced to 0.059 if (033), (222), and (411), the three strongest reflections, are omitted due to the large extinction effect.

A final calculation was made in which the parameters in Table IV were kept constant, and the effective number of atoms at the Ti and O sites were

¹⁶ W. R. Busing and H. A. Levy, Oak Ridge National Laboratory Report Nos. 59-4-37 and 59-12-3, 1959 (unpublished).

TABLE III. Coordinates of Ti₂O₃ at 4.2°K based on isotropic temperature factors.

	x	y	z	B (Å ²)
Ti	0.3456±4 ^a	0.3456±4	0.3456±4	0.326±0.146
O	0.5622±9	0.9378±9	0.2500	0.277±0.149
K (scale factor) = 0.275±0.012				

^a In this and subsequent tables, error values without decimal points correspond to the last significant digits in the function value.

allowed to vary. This is equivalent to measuring the stoichiometry of the sample. The value of R barely changed, from 0.117 to 0.116. The effective formula became Ti_{1.99±0.02}O_{3.00±0.02}, indicating excellent stoichiometry. Photometric analysis (by T. Y. Kometani, Bell Telephone Laboratories) gave Ti as 66.1±0.2%, compared with a calculated value of 66.62%. By difference O is 33.9±0.2%, compared with 33.38% calculated, again indicating good stoichiometry.

REFINEMENT OF THE CRYSTAL STRUCTURE AT 298°K BY X-RAY DIFFRACTION

It is of value to compare the results in Tables III and IV with those obtained by x-ray diffraction at room temperature. Newnham of MIT had already visually measured¹⁷ a set of intensities diffracted by a small cylinder of Ti₂O₃, using a Weissenberg camera and MoK α x radiation, which they kindly allowed me to use. These zero-level (hll) intensities were corrected for absorption and the Lorentz-polarization factors and introduced into a set of least-squares refinement calculations following the pattern established with the neutron data. The coordinates obtained with isotropic temperature factors, using Watson and Freeman's form factor¹⁸ for Ti³⁺ and a modified Berghuis *et al.* form factor¹⁹ for O²⁻, are given in Table V.

The coordinates obtained following three anisotropic temperature factor least-squares refinement, with ORXLS,¹⁶ are shown in Table VI. The coordinates in Table V correspond to $R=0.133$ and in Table VI to $R=0.108$. A calculation to check the stoichiometry of the sample used in the x-ray work did not change the value of R , but indicated the effective formula to be Ti_{2.01±0.01}O_{2.60±0.06}.

INTERATOMIC DISTANCES AT 4.2°K AND AT 298°K

The interatomic distances in Ti₂O₃ at 4.2°K and at 298°K have been computed from the coordinates in Tables IV and VI using the Busing and Levy ORXFE program,¹⁶ and are presented in Table VII. No allowance has been made for thermal motions in this table.

¹⁷ R. E. Newnham and Y. M. de Haas, *Z. Krist.* **117**, 235 (1962).

¹⁸ R. E. Watson and A. J. Freeman, *Acta Cryst.* **14**, 27 (1961).

¹⁹ J. Berghuis, I. J. Bertha, H. Haanappel, M. Potters, B. O. Loopstra, C. H. MacGillavry, and A. L. Veenendaal, *Acta Cryst.* **8**, 478 (1955).

TABLE IV. Coordinates of Ti_2O_3 at 4.2°K based on anisotropic temperature factors.^{a,b}

	x	y	z	β_{11}	β_{22}	β_{33}	β_{13}
Ti	0.3450 ± 2	0.3450 ± 2	0.3450 ± 2	0.0120 ± 12	0.0120	0.0006 ± 1	0
O	0.5625 ± 3	0.9375 ± 3	0.2500	0.0054 ± 8	0.0061 ± 9	0.0010 ± 1	-0.0002 ± 1

^a The temperature factors are given with respect to the hexagonal setting.

^b For Ti, $\beta_{11} = \beta_{22} = 2\beta_{12}$ and $\beta_{23} = \beta_{31} = 0$; for O, $\beta_{22} = 2\beta_{12}$ and $\beta_{23} = 2\beta_{13}$. $K = 0.3226 \pm 73$.

AMPLITUDES OF VIBRATION

The rms components of vibration along the principal axes of the assumed vibration ellipsoid can readily be computed from the β_{ij} of Tables IV and VI by the Busing-Levy ORXFE program.¹⁶ At 4.2°K, the

TABLE V. Coordinates of Ti_2O_3 at 298°K based on isotropic temperature factors.

	x	y	z	B (Å ²)
Ti	0.3447 ± 2	0.3447 ± 2	0.3447 ± 2	0.240 ± 0.037
O	0.5606 ± 25	0.9394 ± 25	0.2500	0.489 ± 0.116

K (scale factor) = 0.087 ± 2

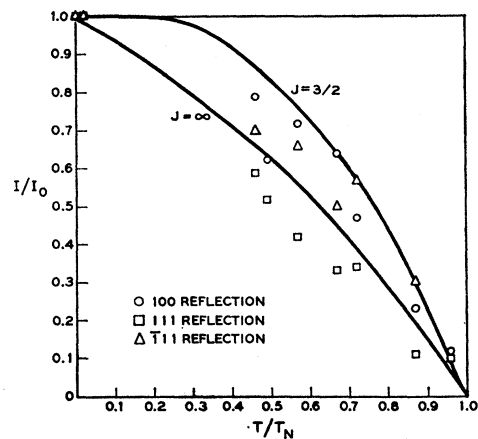
neutron data give for Ti, the rms components 0.075 ± 5 , 0.110 ± 1 , 0.110 ± 7 Å and for O, 0.072 ± 9 , 0.077 ± 6 , 0.098 ± 5 Å. At 298°K, the x-ray data give 0.043 ± 6 , 0.061 ± 1 , 0.062 ± 4 Å for Ti and 0.052 ± 18 , 0.097 ± 22 , 0.118 ± 20 Å for O. The corresponding rms radial vibrational displacements are 0.173 ± 6 for Ti and 0.144 ± 9 Å for O at 4.2°K and 0.097 ± 4 for Ti and 0.161 ± 23 for O at 298°K.

THE MAGNETIC STRUCTURE AT 4.2°K

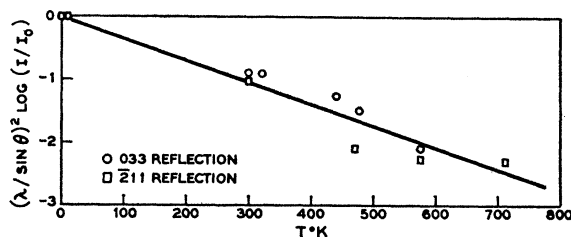
A careful search of the neutron diffraction in the (hll) zone failed to reveal any fractional order reflections, indicating the magnetic unit cell to be identical with the nuclear unit cell. There are, however, 20 independent observed (hll) reflections (see Table II), with the condition $h = 2n + 1$, in violation of the c -glide plane in the nuclear space group $R\bar{3}c$. The series of tests presented in the experimental section lead to the conclusion that these reflections are produced by a magnetic interaction with the neutrons. A final proof of this conclusion would be the observation of a characteristic Brillouin-type temperature dependence for these reflections. The variation of the intensities of (100), (111), and ($\bar{1}\bar{1}\bar{1}$) as a function of temperature is presented in Fig. 1(a) and for comparison, the corresponding variation for the intensities of the nuclear reflections (033) and ($\bar{2}\bar{1}\bar{1}$) in Fig. 1(b). The intensities of (100), (111), and ($\bar{1}\bar{1}\bar{1}$) are observable at temperatures up to 631°K but are unobservable at 689 and 711°K. A Néel temperature of 660°K was, hence, assumed for this crystal and was used in deriving Fig. 1(a). It can be seen from Fig. 1(a) that the average dependence of the "magnetic" intensities upon temperature, although closer to the

theoretical curve for $J = \infty$ than for $J = \frac{3}{2}$, is essentially that predicted by the Brillouin function. The temperature dependence of the "nuclear" intensities, on the other hand, follows the usual Debye behavior.

The transition temperatures previously reported for Ti_2O_3 are about 450 to 600°K: the temperature found by neutron diffraction is considerably higher. The resistivity of the present sample was, hence, measured using the furnace and temperature controller of MacChesney, and the results are given in Fig. 2. The absolute scale of resistivity values in Ω -cm in Fig. 2 is liable to some uncertainty due to the difficulty in accurately estimating the pressure contact areas on the crystal. The transition is seen to be about 450°K wide; the midpoint lies at about 680°K, in good agreement with the neutron diffraction value.



(a)



(b)

FIG. 1. (a) Variation of the intensities of three "magnetic" reflections with temperature, normalized to the intensity at 1.43°K (I_0) and $T_N = 660$ °K. The corresponding Brillouin functions for $J = \frac{3}{2}$ and $J = \infty$ are indicated for comparison. (b) Logarithmic variation of the intensities of two "nuclear" reflections with temperature.

TABLE VI. Coordinates of Ti_2O_3 at 298°K based on anisotropic temperature factors.^a

	x	y	z	β_{11}	β_{22}	β_{33}	β_{13}
Ti	0.3445±2	0.3445±2	0.3445±2	0.0037±5	0.0037	0.0002±1	0
O	0.5585±26	0.9415±26	0.2500	0.0104±28	0.0135±47	0.0003±2	-0.0002±4
				$K=0.0888±17$			

^a See footnote b to Table IV.

The establishment of the measured structure factors in Table II as being unambiguously magnetic in origin now permits consideration of the three most probable

TABLE VII. Interatomic distances less than 3.1 Å at 4.2°K and at 298°K.

	At 4.2°K (Å)	At 298°K (Å)
Ti—O	2.024±6	2.037±8
Ti—O	2.066±6	2.046±12
Ti—Ti	2.592±9	2.578±9
Ti—Ti	2.990±11	2.988±12
O—O	2.787±11	2.751±24
O—O	2.792±7	2.782±9
O—O	2.883±7	2.890±8
O—O	3.070±12	3.089±18

antiferromagnetic ordering schemes proposed by Shull *et al.*²⁰ for the similar case of α Fe_2O_3 . Assuming the moments are associated with the Ti^{3+} ions, the senses of these moments at cation positions along the rhombohe-

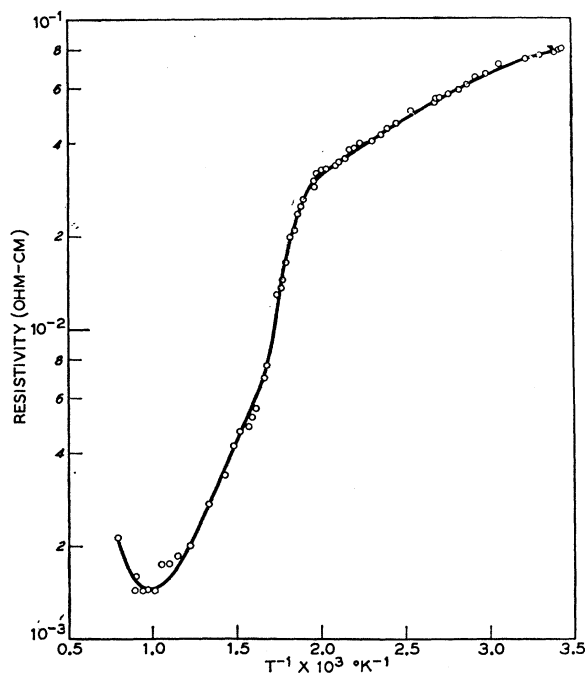


FIG. 2. Resistivity of Ti_2O_3 crystal used for the neutron diffraction measurements vs reciprocal temperature.

²⁰ C. G. Shull, W. A. Strauser, and E. O. Wollan, *Phys. Rev.* **83**, 333 (1951).

dral $[111]$ axis, for these three cases, can be as illustrated in Fig. 3.

Scheme (a) corresponds to α Fe_2O_3 between 253 and 948°K, (c) to Cr_2O_3 , and at present no known magnetic structure corresponds to (b). It should be noted that the crystal inversion centers in (a) lie between parallel moments. The unit cell shown by Shull *et al.*²⁰ uses an origin $\frac{1}{4}, \frac{1}{4}, \frac{1}{4}$ from the inversion center, with a resulting value for u_{Fe} in (4c) of 0.105; this is equivalent to $0.105 + \frac{1}{4} = 0.355$ if the inversion center is taken as origin. If no regard is taken of the inversion centers, the ordering sequence in schemes (a) and (b) is equivalent.

The observation of the structure factors given in Table II immediately rules out model (c), for in this case (hll) could reflect only for $h=2n$. In case (a), the crystal structure factors have the form $4p \cos[2\pi \times (hu+ku+lu)]$ and in (b), $-4p \sin[2\pi(hu+ku+lu)]$, where p is the magnetic scattering amplitude. We may consider two further subdivisions of models (a) and (b). In (i), the moments may be either parallel to the $[111]$ axis, hence retaining the nuclear trigonal symmetry,

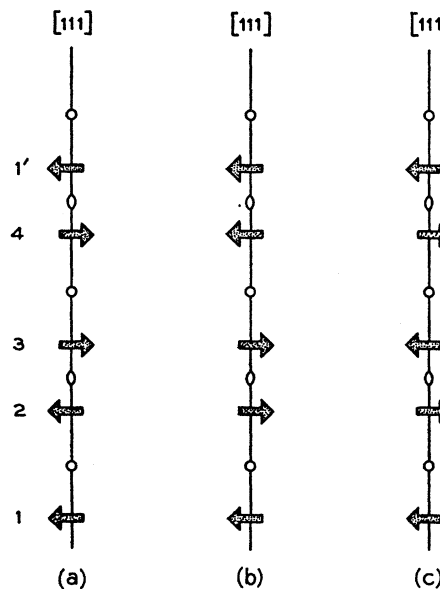


FIG. 3. Arrangement of the moments of four cations along the $[111]_R$ at (1) $u-\frac{1}{2}, u-\frac{1}{2}, u-\frac{1}{2}$; (2) $\frac{1}{2}-u, \frac{1}{2}-u, \frac{1}{2}-u$; (3) uuu ; (4) $\bar{u}\bar{u}\bar{u}$. The open circles represent inversion centers, the ellipses twofold axes either normal to or in the plane of the figure. (a) corresponds to Ti_2O_3 and α Fe_2O_3 , (b) is unknown, (c) corresponds to Cr_2O_3 .

or (ii), they may be inclined to this axis. In case (i), $F(111)$ and $F(333)$ should be zero, contrary to observation, which thus eliminates models with moments along $[111]$. In case (ii), following the symmetry arguments of Vonsovsky and Turov,²¹ the magnetization direction can either lie in the c -glide plane or else be parallel with a twofold axis normal to $[111]$. Small departures from either perpendicular direction can, in principle, give rise to "weak" ferromagnetism, as indeed is observed in α Fe_2O_3 . The small magnetic susceptibility of Ti_2O_3 below T_N of about 1×10^{-6} cgs g^{-1} does not indicate appreciable ferromagnetism, except possibly at very low temperatures.²² For the analysis of the data in Table II, we now assume that the macroscopic trigonal symmetry is maintained, in the absence of an external magnetic field, by domain formation. In a given domain, if the elementary magnetization vector makes an angle φ with a twofold axis in the plane normal to $[111]$, then in the other two equally populated sets of domains, the corresponding angles will be $\varphi \pm 120^\circ$. Because of this angular relationship, the angle φ is indeterminate from the data in Table II. The "magnetic" structure factors may now be calculated, based on the Ti^{3+} ion position in Table IV, and with the observed values in Table II on the absolute scale ($\pm 2.3\%$) provided by the analysis of the nuclear structure factors.

The magnetic structure factor, assuming a spin contribution only, is given by $0.2695 \times \sin \alpha \times 2S \times f \times 4 \times \left[\frac{\cos \alpha}{\sin \alpha} \right] 2\pi(hu + kv + lw)$, where α is the angle between the magnetization and the scattering vectors, S is the effective spin quantum number, f is the spin-only form factor, and u is the position coordinate for the $3d$ electron. Initial calculations clearly showed that the free-ion form factor for the $3d^1$ electron configuration in Ti^{3+} as computed by Watson and Freeman,¹⁸ assuming complete quenching of the orbital momentum, was not applicable to Ti_2O_3 . The term $2Sf$ can be replaced by $Lf_L + 2Sf_S$, where L and S are the effective orbital and spin quantum numbers and f_L and f_S are the corresponding L and S form factors. By equating F_{meas} to the calculated magnetic structure factor for each reflection, values for $(Lf_L + 2Sf_S)$ as a function of $(\sin \theta)/\lambda$ were obtained. The average of these values gave an effective composite form factor which increases with $(\sin \theta)/\lambda$, from 0.208 at $(\sin \theta)/\lambda = 0.1 \text{ \AA}^{-1}$ to a maximum value of 0.330 at $(\sin \theta)/\lambda = 0.7 \text{ \AA}^{-1}$. This composite form factor was used to evaluate F_{calc} (a) and F_{calc} (b) in Table II, where (a) and (b) refer to the ordering schemes in Fig. 3. The agreement for model (a) is so much better than for (b) than the latter may reasonably be excluded. The values for R are 0.37 for (a) and 0.62 for (b). In addition, the ratio of $F_{\text{meas}}:F_{\text{calc}}$ exceeds 4:1 for four reflections in

case (b). The agreement for case (a) is improved further by assuming the $3d$ electron is located at $u=0.335$ instead of 0.3451. This case is indicated as F_{calc} (a-1) in Table II. R is reduced to 0.235 for model (a-1) and the largest disagreement becomes $F_{\text{meas}}:F_{\text{calc}}$ for $F(522)$ with a value of 1:1.8.

The moment to be assigned to the Ti^{3+} cation may now be determined from the quantity $(Lf_L + 2Sf_S)$ by extrapolation to zero scattering angle of the smoothed function vs $(\sin \theta)/\lambda$. At $(\sin \theta)/\lambda = 0$, $f_L = f_S = 1$ and $\mu_{\text{eff}} = L + 2S = 0.2$ Bohr magnetons. The experimental scatter about the smoothed $Lf_L + 2Sf_S$ function is about $\pm 10\%$ at low-scattering angles and about $\pm 40\%$ at the largest observed angles. A detailed explanation for the shape of this function has been given by Blume.²³ This is based on the spin and orbital momenta being taken antiparallel, and uses effective values for L and S obtained from crystal field calculations for the Ti^{3+} ion in a trigonal field. The form factor is then $(0.78f_L - 0.66f_S)/0.12$, where Watson and Freeman's value¹⁸ is used for f_S and a new Ti^{3+} orbital form factor²⁴ is used for f_L .

On the basis of model (a), it is now possible to assign the most likely Shubnikov space groups. Reference to Fig. 3(a) shows that the moments on cations 1 and 2 are related by a normal inversion center (since the moments have the symmetry of axial vectors). There are two possible orientations of the moments in model (a) with respect to the twofold axis and the glide plane normal to this axis. If the twofold axis is normal to the paper in Fig. 3(a) and lies between cations 2 and 3 (and 4 and 1'), this orientation will have as symmetry operators a twofold axis and the c -glide plane with translation $[111]/2$ resulting in $2/c$. If the twofold axis is in the plane of the paper the resulting symmetry is $2'/c'$. No distinction can be made between the symmetry elements $2/c$ and $2'/c'$ on the basis of the present data: these elements together with the inversion center constitute the entire array of symmetry operators. This may now be combined with the lattice C centering to describe the magnetic space group as $C2/c$ or $C2'/c'$.

The nuclear scattering density along the $[111]$ axis passing through the Ti^{3+} ion is shown in Fig. 4 (lower curve). The corresponding magnetic moment density through the $3d$ electron associated with the Ti nucleus is shown in the middle curve of Fig. 4. The upper curve shows the over-all electron density in Ti^{3+} , measured by x-ray diffraction. The differences between the nuclear position, measured at 4.2°K and the complete electron cloud measured at 298°K is slightly greater in the curves of Fig. 4 than in Tables IV and VI. This is most probably caused by Fourier series termination effects, particularly in the neutron diffraction case. The difference in Ti-coordinate obtained by least squares based

²¹ S. V. Vonsovsky and E. A. Turov, J. Appl. Phys. **30**, 9S (1959).

²² P. H. Carr and S. Foner, J. Appl. Phys. **31**, 344S (1960).

²³ M. Blume (to be published).

²⁴ A. J. Freeman (private communication).

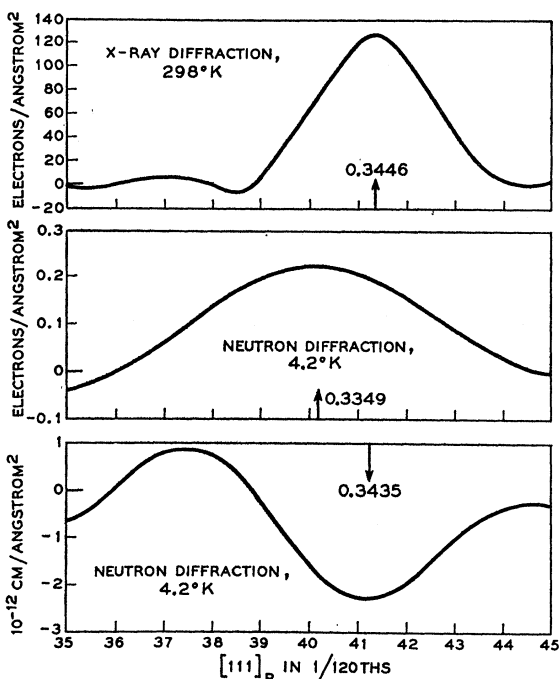


FIG. 4. (Upper) Profile through the complete electron density of a Ti^{3+} cation in Ti_2O_3 at 298°K along $[111]_R$. (Middle) Profile through the magnetic moment density at 4.2°K . (Lower) Profile through the nuclear scattering density at 4.2°K . The negative scattering length of Ti causes a negative density.

on the x ray and the neutron method is $\Delta u = 0.0005$ or 0.007 \AA , and by use of Fourier series is 0.015 \AA . The value 0.3450 from Table IV is probably the best value for the Ti^{3+} position with which to compare the magnetic moment position in Fig. 4 of 0.3349 . The difference of 0.138 \AA is too large not to be significant, although the error in the middle curve of Fig. 4 has not been evaluated. This error is unlikely to be more than 0.04 \AA . The density maxima of the opposed moments hence appear closer together than their associated nuclei. It is also significant that the moment density is much more diffuse than the electron or the nuclear scattering densities.

DISCUSSION

The present study has unambiguously demonstrated the antiferromagnetic nature of the phase below the Néel temperature in Ti_2O_3 . The ordered array of moments in this corundum-type structure is similar to that in $\alpha\text{-Fe}_2\text{O}_3$ in the temperature range 253 to 948°K . The crystal structure consists of a slightly distorted hexagonal closest packing of O^{2-} ions, with the Ti^{3+} occupying half of the nearly regular octahedral interstices. Magnetically, the structure contains puckered sheets of ferromagnetically coupled Ti^{3+} cations, with moments in the rhombohedral (111) planes, separated by the O^{2-} sheets. The moments in any cation sheet are antiparallel to those in the next cation sheet.

The primary antiferromagnetic interaction is between pairs of Ti^{3+} cations lying on the trigonal axis and separated, at 4.2°K , by a distance of 2.592 \AA . The arrangement of nearest neighbor O^{2-} is shown in Fig. 5(a), and consists of a pair of trigonal antiprisms sharing a common triangular face, with an O—O separation of 2.787 \AA . The six nearest O^{2-} around each Ti^{3+} can, of course, be more usually described as forming a slightly distorted octahedron, with three Ti—O distances of 2.024 \AA and three others of 2.066 \AA . At room temperature, the distortion is less with corresponding Ti—O distances of 2.037 and 2.045 \AA . The Ti^{3+} in Fig. 5(a) is 0.975 \AA from the plane of the upper three O^{2-} , and 1.297 \AA from the plane of the three O^{2-} common to both octahedra. The secondary Ti^{3+} — Ti^{3+} interaction is ferromagnetic, and is between cations 2.990 \AA apart: these cations lie in planes separated by an 0.322 \AA distance. The arrangement of ferromagnetically coupled pairs of Ti^{3+} and their nearest neighbors is shown in Fig. 5(b): these octahedra share edges.

The orientation of the moments perpendicular to the trigonal axis, and the small magnitudes of these Ti^{3+} moments have interesting implications. In the $3d^1$ configuration for the free Ti^{3+} ion, $S = \frac{1}{2}$ and $L = 2$. In the crystal field present which is primarily cubic, the fivefold orbital degeneracy of the 2D state is lifted into an upper e_g doublet and a lower t_{2g} triplet, with a separation of about $20\,000 \text{ cm}^{-1}$. The smaller trigonal field now splits the triplet into a t_{\pm} doublet and a t_0 singlet. The spin-orbit coupling in turn splits the t_{\pm} doublet: for Ti^{3+} in corundum the splitting is reported²⁵ to be small, about 35 cm^{-1} . In the Ti^{3+} -doped corundum case, g_{\perp} has been reported²⁶ less than or equal to 0.1 ; g_{\parallel} to be 1.067 . It is not clear whether the t_{\pm} doublet is

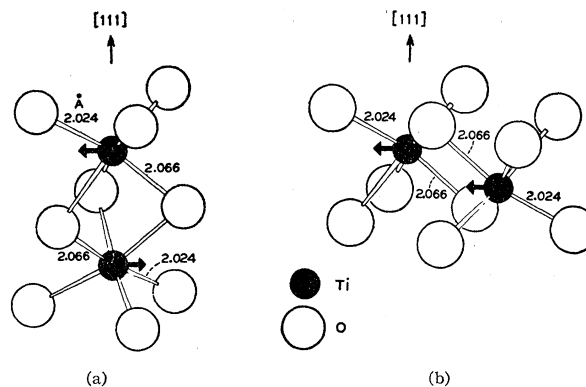


FIG. 5. (a) Oxygen octahedra surrounding antiferromagnetic pair of Ti^{3+} , sharing a face, (b) Oxygen octahedra surrounding ferromagnetic pair of Ti^{3+} , sharing an edge. For each Ti^{3+} in (b) there are two additional Ti^{3+} , forming an infinite puckered sheet. The arrows represent the moment directions.

²⁵ L. S. Kornienko and A. M. Prokhorov, First International Conference on Paramagnetic Resonance, Israel, 1962 (unpublished).

²⁶ L. S. Kornienko and A. M. Prokhorov, Zh. Eksperim. i Teor. Fiz. **38**, 1651 (1960) [translation: Soviet Phys.—JETP **11**, 1189 (1960)].

lower than the t_0 singlet in Ti_2O_3 , as has always been found for transition metal ions in corundum, or higher as recently reported for Cr_2O_3 .²⁷ In addition, the antiferromagnetic exchange splitting is likely to be comparable with the spin-orbit splitting in view of the high Néel point. It should be pointed out here that the behavior of Ti^{3+} substituted into the corundum lattice only approximates that of Ti^{3+} in pure Ti_2O_3 . Although the two crystals are isomorphous, in Al_2O_3 the hexagonal lattice constants are $a=4.76$, $c=12.99$ Å whereas in Ti_2O_3 , $a=5.15$ and $c=13.64$ Å. The nearest O^{2-} neighbors around each Ti^{3+} ion in the corundum lattice are 1.86 and 1.97 Å distant; in Ti_2O_3 these distances are 2.024 and 2.066 Å at 4.2°K. The nearest cation neighbors in corundum are *aluminum* at distances of 2.65, 2.97, 3.22, 3.50, and 3.85 Å; in Ti_2O_3 they are *titanium* at corresponding distances of 2.59, 2.99, 3.56, 3.74, and 4.23 Å. Even disregarding the different nuclei and polarizabilities in the two cases, a simple point-charge model would not give identical fields at the Ti^{3+} site.

On the basis of Blume's analysis,²³ the neutron diffraction results can be explained if the sign of the trigonal field splitting is taken as negative, with the doublet higher. If this separation v is 200 cm^{-1} and the spin-orbit coupling is 100 cm^{-1} , then the average value for L_x is 0.78 and for $2S_x$ is 0.66. This would predict a moment of $0.12\mu_B$ and reasonably reproduce the observed form factor curve. Qualitatively, the small value for the observed moment of $0.2\mu_B$ and the large exchange field corresponding to $T_N \approx 660^\circ\text{K}$ are consistent with the small measured magnetic susceptibility, both \perp and \parallel to the trigonal axis.

Finally, the relationship should be pointed out between the magnetic symmetry found in antiferromagnetic Ti_2O_3 and the crystallographic symmetry reported²⁸ in V_2O_3 below the transition temperature of 170°K . In Ti_2O_3 , the ordering of the magnetic moments

normal to the trigonal axis destroys that symmetry element, but the diad normal to the c -glide plane is retained in the magnetic space group $C2/c$ (or $C2'/c'$). In V_2O_3 , Warekois has shown by x-ray powder photography that below 170°K , the rhombohedral symmetry is lowered to monoclinic. The unit cell he proposed does not form a monoclinic Bravais lattice but transformation of his monoclinic a axis $\approx \mathbf{a}_{\text{Hex}} + 2\mathbf{a}_{\text{Hex}} = \sqrt{3}a_{\text{Hex}}$ with $\beta \approx 90^\circ$, to a new monoclinic a axis $\approx \mathbf{a}_{\text{Hex}}/\sqrt{3} + 2\mathbf{a}_{\text{Hex}}/3 - 2\mathbf{c}_{\text{Hex}}/3$, with $\beta \approx 164.4^\circ$, gives a cell isomorphous with that of antiferromagnetic Ti_2O_3 . Both low-temperature crystals, hence, belong to the space group $C2/c$ (or $C2'/c'$). In V_2O_3 , $a=9.69$, $b=4.98$, $c=13.88$ Å and $\beta=164.4^\circ$, and in Ti_2O_3 , $a=9.57$, $b=5.15$, $c=13.64$ Å and $\beta=161.9^\circ$. The general similarity in the physical properties of V_2O_3 above and below 170°K of those of Yi_2O_3 above and below its Néel point strongly suggest that the transition of V_2O_3 is also from a paramagnetic metallic conductor to an antiferromagnetic semiconductor. The large difference between the two Néel points and the greater distortion in atomic positions in ordered V_2O_3 than in Ti_2O_3 , leading to crystal rupture in V_2O_3 are probably related, although a detailed mechanism is at present lacking.

ACKNOWLEDGMENT

It is a pleasure to thank F. A. Barbieri for orienting and grinding the single-crystal cylinder of Ti_2O_3 , E. J. Loeser for operating SCAND and F. E. Wallenquest for processing the intensity data from SCAND, Dr. J. B. MacChesney for use of his furnace and advice on the resistivity measurements, and J. L. Bernstein for assistance with these measurements and for measuring the density of Ti_2O_3 pycnometrically, Dr. R. E. Newnham for communicating his x-ray measurements, Dr. M. Blume for discussions of the orbital contribution to the neutron magnetic form factor and for making his unpublished values for L_x and S_x available, and Dr. S. Geschwind for discussions on crystal-field theory.

²⁷ K. A. Wickersheim, Suppl. J. Appl. Phys. **34**, 1224 (1963).

²⁸ E. P. Warekois, J. Appl. Phys. **31**, 346S (1960).